

***Ab initio* study of the effect of solute atoms on the stacking fault energy in aluminum**

Yue Qi\* and Raja K. Mishra

*GM R&D Center, MC:480-106-224, 30500 Mound Road, Warren, Michigan 48090-9055, USA*

(Received 11 December 2006; revised manuscript received 16 February 2007; published 6 June 2007)

The stacking fault energy (SFE) in binary and ternary alloys of Al with common alloying elements was studied using density functional theory. Among these alloying elements, Fe further increases the SFE and Ge reduces the SFE of Al. The alloying elements increase the SFE by increasing the directional inhomogeneity in the electronic charge distribution of Al. The maximum value of charge difference on the fault plane,  $\text{Max}(\Delta\rho)$ , is used to characterize how many electrons have been redistributed due to the stacking fault formation, and the SFE increases with  $\text{Max}(\Delta\rho)$ .

DOI: [10.1103/PhysRevB.75.224105](https://doi.org/10.1103/PhysRevB.75.224105)

PACS number(s): 61.72.Nn, 62.20.Fe, 71.15.Nc

**I. INTRODUCTION**

Plastic deformation in metals is mediated by dislocation generation, movement, and interaction. The overall ductility is a microstructure-sensitive property,<sup>1</sup> governed by interactions between dislocations with solutes, vacancies, other dislocations, grain boundaries, and secondary phases. Fundamental studies of dislocation energetics and their generation, multiplication, and annihilation processes could provide guidelines for alloy or process modifications to optimize microstructure for ductility enhancement. In Al alloys, forest dislocation networks on nonintersecting slip planes contribute to nonhomogeneous slip distribution, easy shear localization, and premature failure. One approach to distribute slip homogeneously is to fundamentally alter the slip behavior by lowering the stacking fault energy (SFE) of Al alloys so that easy glide of dislocations is replaced by entanglement of partial dislocations and formation of stacking fault tetrahedra.<sup>2</sup>

The effect of SFE on dislocation slip in fcc metals is well known.<sup>3</sup> Dislocations in metals and alloys reduce their elastic energy by separating into two partial dislocations which are joined by a band of faulted structure in the slip plane, called a stacking fault. The equilibrium width of such an extended dislocation depends on the characteristic SFE of the material. To allow a dislocation to cross-slip onto a new slip plane, the partial dislocations must be forced together followed by a resplit on the new slip plane. Thus, lower SFE corresponds to larger partial separation and more difficult cross slip for the partials, favoring a three-dimensional network of sessile and glissile dislocations. Such a network formation delays shear band formation and premature localization as seen in Cu, Ag, etc. In contrast, higher SFE leads to narrower dislocation separation or undissociated dislocations in Al, which tends to form forest dislocation networks without appreciable sessile dislocations pinned by jogs and kinks.<sup>1,4</sup> Easy glide results in easy slip band formation. These bands act as soft zones for dislocations to move as deformation proceeds, which localizes the deformation in these bands in single grains and accelerates shear band formation in an aggregate of grains, leading to failure.

The differences in SFE of fcc metals like Al, Cu, and Ag arise from the differences in their electronic structures. Al has  $2s^2 2p^1$  valence electrons, but Cu has a fully occupied  $3d$  orbital and  $4s^1$  electron. Using density functional theory calculations, Ogata *et al.*<sup>5</sup> have shown that while the charge

density distribution is nearly spherical in fcc metals like Cu and Ag, the pocket of charge density at the octahedral interstice in Al has a cubic symmetry and is angular in shape due to the slight covalent and directional nature of bonding.<sup>6</sup> When an intrinsic stacking fault is created by shearing the close-packed plane along  $\langle 112 \rangle$ , the electrons can redistribute well in the nondirectionally bonded metals like Cu and Ag without a large energy penalty. However, the electrons do not readapt so readily in Al due to the directionality of the bonds, resulting in large SFE. Experimentally it is known that the SFE in Al is much larger than that in Cu, Ag, or even Ni which shows bond directionality due to magnetic spin contributions.<sup>6</sup>

If alloying can change the SFE and favor dislocation dissociation in Al alloys, new mechanisms of slip evolution can improve their ductility. Previous searches for alloying addition to reduce the SFE of Al have not been very successful. Reported experimental values of SFE are unreliable because of inaccuracies in measuring small differences in the separation distance between partial dislocations in electron microscope images. Theoretical values of SFE in Al and Al alloys vary widely in the literature, partly because of inaccuracies in modeling electronic interactions between atoms using an empirical potential (EP),<sup>7</sup> such as the embedded atom potential (EAM) potential,<sup>8</sup> glue potential,<sup>9</sup> or phenomenological  $n$ -body potential.<sup>10</sup> This report presents a first-principles simulation of alloying effects on the SFE to provide limiting case values that can serve as a guide to future experimental search for alloy design to lower the SFE and distribute slip homogeneously. One of the greatest advantages of first-principles electronic structure methods over those utilizing an empirical potential is the incorporation of electronic exchange and correlation effects which account for the interaction of electrons in condensed matter. More importantly, for many alloying elements in our calculation, the empirical potential is simply not available.

The aim of this paper is to investigate the effect of small additions of alloying elements that could alter the anisotropic electron distribution around Al atoms towards spherical symmetry, consequently reducing the SFE and altering the slip mechanism. Even though quantitative experimental data on Al SFE are scarce,<sup>11,12</sup> indirect evidence of lower SFE in Al alloys has been reported for Cr and Mg additions.<sup>13,14</sup> In this investigation, first-principles calculations of changes to the electron distribution and SFE with the addition of common alloying elements in binary and ternary Al alloys have been

carried out for revealing the trends in electron configuration changes. The SFE values calculated here are valid at absolute zero and can be considered as an upper limit to establish trends rather than being suitable for comparison with existing experimental data. Calculations including the temperature effect and full dislocation structures for experimental validation will be presented in the future.

## II. METHODS

The *ab initio* calculations are based on density functional theory (DFT) implemented in the Vienna *ab initio* simulation package (VASP).<sup>15,16</sup> The generalized gradient approximation (GGA) of Perdew and Wang<sup>17</sup> is used for the exchange-correlation energy function. For Al and Mg, a norm-conserving pseudopotential<sup>18,19</sup> is used. For the other solute atoms, an ultrasoft pseudopotential<sup>20</sup> is chosen. Total energies of the optimized structures are computed with the linear tetrahedron method with Blöchl-Jepsen-Andersen<sup>21</sup> corrections in order to eliminate any broadening-related uncertainties in the energies. Ground-state atomic geometries are obtained through minimization of the Hellman-Feynman<sup>22</sup> forces using a conjugate gradient algorithm.<sup>23</sup> For all structures, the electronic degrees of freedom are converged to  $10^{-5}$  eV/cell and the Hellman-Feynman forces are relaxed to less than 0.05 eV/Å. A total energy convergence of 1–2 meV/atom is obtained with a 270 eV plane-wave cutoff energy, which is also valid for all alloying elements in the calculation. As a check of the computational methodology, we computed selected bulk properties and surface properties of crystalline Al. For the primitive cell of fcc Al, a Monkhorst *K*-point grid of  $10 \times 10 \times 10$  gave a good energy convergence of 0.001 eV/atom. The calculated bulk properties of  $a=4.04$  Å,  $B=72.1$  GPa, and  $E_{coh}=3.56$  eV (lattice parameter, elastic modulus, and cohesive energy, respectively) compare well with experiment values of  $a=4.05$  Å,<sup>24</sup>  $B=72.2$  GPa,<sup>25</sup> and  $E_{coh}=3.39$  eV.<sup>26</sup>

The SFE for Al is calculated with a slab model. In this model ten layers of Al(111) planes (with three atoms per plane for most cases) are stacked in a supercell and a  $10\text{-}\text{Å}$  vacuum is added in order to avoid interactions with periodic images. A  $\gamma$ -centered *K*-point grid of  $10 \times 10 \times 1$  for the hexagonal supercell gives a converged surface energy of  $0.78$  J/m<sup>2</sup> (0.27 eV/surface atom). The stacking fault structure is constructed by shifting the top five (111) layers by a distance of  $a/\sqrt{6}$  along  $\langle 112 \rangle$  direction ( $-y$  direction of the supercell), to form an *ABCABABCAB* packing from a perfect fcc packing of *ABCABCABCA*. The SFE is defined as the energy difference between the faulted structure and the perfect fcc structure. To eliminate the free surface effect on the computed SFE, tests with different slab thickness in the range 8–12 layers were used and it was determined that ten layers of (111) planes gave convergence of 0.01 J/m<sup>2</sup> of SFE.

The alloying is created by substituting one Al atom at the stacking fault plane, the fifth atomic layer, with a solute atom. Solute atoms chosen in this study are Mg, Fe, Mn, Cr, Cu, Zn, Ga, Ti, and Ge. The concentration of the solute atom turns out to be 3.3% for the whole system, but at the stacking

fault plane, the concentration corresponds to 33% monolayer coverage (atomic concentration in one plane). Larger supercells—for example, having 25% monolayer coverage at the stacking fault plane—gave a value closer to the SFE of pure Al due to decreasing concentration. A similar trend was found in the calculations of Lu *et al.* on H effects on SFE of Al, where they tested 100%, 33%, and 25% monolayer coverage of H atom at the stacking fault plane.<sup>27</sup> Although the concentration is high for the solute atom at the stacking fault, it amplifies the alloying effect on the SFE, giving an estimation of the trend of SFE changes upon alloying. We also calculated the combination of two common alloying elements for Al—namely, Si with Mg and Si with Cu normally found in commercial alloys. The two alloy elements substitute for the Al atoms at the stacking fault plane, and the corresponding monolayer coverage is 66%. These combined alloying effects are compared to the cases with only a single element at the same concentration.

The SFE changes when the atom is located at one layer away from the stacking fault, which results in a slightly lower SFE for Mg substitution and higher SFE for Fe and Cr substitutions compared to the structure with the solute atom on the stacking fault plane. In other words, for Fe and Cr solute atoms, it is energetically preferable to locate them at the stacking fault plane compared to locating them farther away from the fault plane. For Mg, it is preferable to locate the solute atom next to the stacking fault. But the difference in energies for Mg located at or next to the stacking fault is only 0.5 mJ/m<sup>2</sup>; therefore, in the following discussion we have used the SFE values for Mg when the atom is placed at the stacking fault plane so that the values of SFE for different alloying elements can be compared by keeping the same configuration.

## III. RESULTS AND DISCUSSIONS

### A. Stacking fault energy

Table I lists the calculated SFE values for pure Al and pure Cu, as well as various Al alloys with alloying atoms at the stacking fault plane. The calculated SFEs for pure Al and pure Cu are comparable to the available experimental data. The results also compare well with other published DFT calculation results. Ogata *et al.* have calculated a SFE of 158 mJ/m<sup>2</sup> for Al and 39 mJ/m<sup>2</sup> for Cu (using a 10–12-layer slab model with two atoms per layer).<sup>5</sup> The data in Table I show that with only one solute atom (33% coverage) at the stacking fault, Fe and Mn increase the SFE, while Mg, Si, Ga, Ti, and Ge decrease the SFE. The effect of Cu, Cr, and Zn on the SFE is relatively small, since the calculated changes to SFE values are within the calculation convergence level of  $\sim 10$  mJ/m<sup>2</sup>. It is to be noted that an element like Cu, which has a low SFE, but when placed in the fcc lattice of Al, does not alter the SFE of Al. The lowest SFE (42% reduction of the SFE) for Al is achieved by mixing Al with a Ge atom and the highest SFE (52% increase of SFE) was calculated for Al with Fe. With two solute atoms (66% coverage), the SFE is further reduced by adding the second solute atom for Si and Mg, which already reduce the SFE by one substitution. Although the Cu atom does not change the

TABLE I. Calculated stacking fault energy.

	System	SFE (mJ/m <sup>2</sup> )
	Pure Al	142 (exp 166) <sup>a</sup>
	Pure Cu	33 (exp 45) <sup>a</sup>
33% monolayer coverage at the stacking fault	Fe+Al	216
	Mn+Al	194
	Cr+Al	154
	Cu+Al	142
	Zn+Al	127
	Mg+Al	118
	Si+Al	117
	Ga+Al	113
	Ti+Al	104
	Ge+Al	82
66% monolayer coverage at the stacking fault	SiCu+Al	109
	SiMg+Al	94
	SiSi+Al	105
	MgMg+Al	91
	CuCu+Al	163

<sup>a</sup>Reference 31.

SFE much by one substitution, with the second substitution atom, the SFE actually increased. The combined effect of different alloy elements is not clear. For Si and Mg, the SFE falls between the single alloying mixing at the same concentration. For Si and Cu, the SFE is closer to Si substitution with the same concentration. Therefore the effect of Cu in changing the SFE is very small.

**B. Homogeneous or nonhomogeneous charge distribution**

As proposed by Ogata *et al.*,<sup>5</sup> the high SFE of Al and low SFE of Cu have their origin in their electronic structures. The charge density around Al is more directional than Cu. They have shown that the charge-density isosurface has an inhomogeneous charge distribution in Al (especially at the interstitial regions) and a spherical homogeneous charge distribution in Cu. With a contour plot of the charge density distribution on the (111) plane from the perfect crystal structure, we can easily visualize the isosurface changing its shape in two dimensions (2D). To be able to compare different systems, the absolute charge density  $\rho_0$  (electron/Å<sup>3</sup>) is normalized by the average valence electrons of the system (for example: 3 for Al and 11 for Cu). As shown in Fig. 1, comparing the charge distribution for Al and Cu, one can easily see the spherical nature of charge distribution in Cu and a hexagonal charge distribution around Al atoms. If the alloying atoms can change the charge distribution, it might change the SFE. To prove this concept we compare the charge density at the same plane with substitutions of Fe and Ge, which give the largest and the smallest SFE, respectively. Around the Fe atom, the charge density has a hexagonal pocket shape. More importantly, the large charge distribution not only localizes at the interstitial region, but also

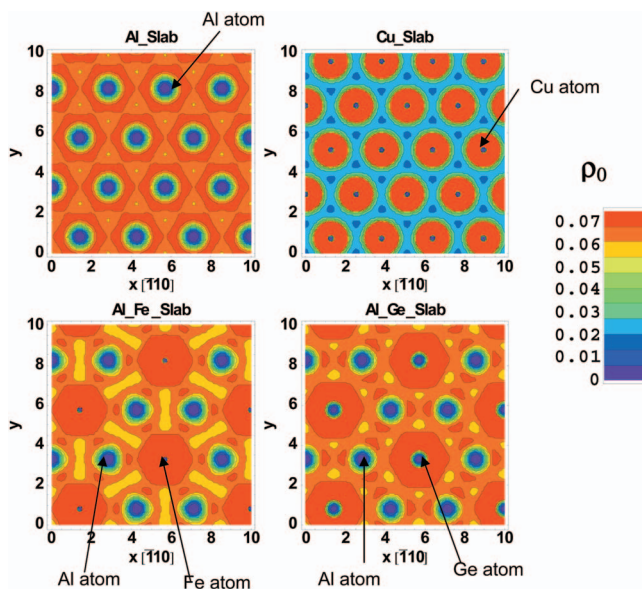


FIG. 1. (Color) The charge density  $\rho_0$  normalized by the number of valence electrons at the fifth (111) plane of the perfect fcc structure. For Al\_Fe\_slab and Al\_Ge\_slab, this plane contains the solute atom.

shows a rodlike shape linking the two Fe atoms, indicating a much more directional bond than what was found in pure Al. The effect of Ge on the shape of the charge density around Al atoms is opposite to that of Fe. The spherical pocket around the Al core is surrounded by a more uniform distribution of charge, instead of being enclosed by a hexagonal pocket. There is less charge localization around the interstitial sites, which indicates that Ge changes the directional bonding between Al into a more homogeneous bonding.

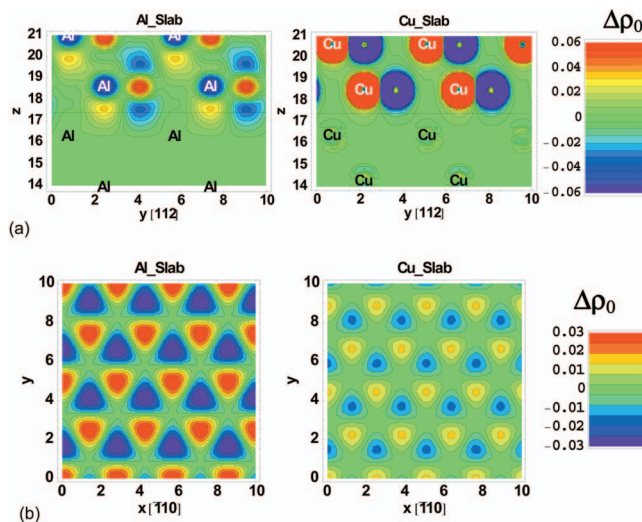


FIG. 2. (Color) (a) Charge density change  $\Delta\rho_0$  due to stacking fault formation on the cross section of (110) plane for pure Al and Cu. The atomic positions of the faulted structure (after shifting) are marked by their elements. (b) The charge density change  $\Delta\rho_0$  on the CDPF, which is the middle plane between the shifted and non-shifted planes [noted as the straight lines in (a)].

### C. Correlation between charge density redistribution and SFE

The shape description of the electron distribution is a qualitative description of the local change of electron density due to alloying. The connection of the SFE with charge density is not straightforward. Since the charge density is a scalar field, changes in the associated energy induced by a defect (stacking fault in this case) result from the changes in the whole field. Kioussis *et al.*<sup>28</sup> attempted to connect the characters of specific charge density critical points (cps) with SFE. They connected the SFE of Al, Ag, and Ir with the charge density and the curvatures of charge density along three principal directions. But their work did not establish a quantitative connection between charge density and SFE.

Here we took a different approach to reveal the influence of changes in the electron density due to stacking fault formation. First, considering that the SFE is defined as the energy difference between the faulted and perfect fcc structure, and the energy difference is due to the electron redistribution caused by shifting of the (111) planes, we have plotted the charge density difference  $\Delta\rho_0$  between the faulted structure and the unfaulted structure. Figure 2(a) shows the change in charge density on the cross section of a (110) plane upon stacking fault formation. The red and yellow regions gain charge while the blue and purple regions lose electrons after the fault is formed. The atomic positions of the stacking fault structure are marked with the element. As the upper slab is shifted by  $a/\sqrt{6}$  ( $[112]/6$ ) along the  $-y$  direction, we see the original positions of these atoms gaining the most electrons, while the new positions of these atoms losing the most electrons. The bottom nonshifted layers have little charge transfer, indicated by the almost featureless pattern of zero change. Between the shifted layers and the nonshifted layers, marked as a straight line in Fig. 2(a), we see the second largest regions of charge gain and loss in Al. In contrast, very little change in the electron distribution on this plane for Cu is observed, since most of its electron density remains spherical. This difference is caused by the more directional bonds in Al compared to that in Cu. The highest charge difference outside the core area is around the midplane between the shifted layer and the nonshifted layer on either side of the fault. Actually this plane should be considered as the charge density fault plane (CDFP), since the two atomic layers above and below this plane are symmetric stacking fault atoms. This fault plane is also the plane where most of the charge density cps appear, as described by Kioussis *et al.*<sup>28</sup> The charge transfer on this fault does not only characterize the directionality of the bond, but also can be correlated to the value of SFE.

Figure 2(b) shows the charge density difference on CDFP, the middle plane between the shifted layer and the nonshifted layer, marked as a straight line in Fig. 2(a). The charge gain and loss on this plane indicates the bond forming and breaking process between the shifted and nonshifted atoms due to stacking fault formation. At any given point on this plane, the maximum value of the charge gain and loss in Al is about  $\pm 0.03/\text{\AA}^3$  and the maximum value of charge gain and loss in Cu is about  $\pm 0.015/\text{\AA}^3$ , which is much smaller than that of Al. Kioussis *et al.* also provide the absolute charge density change during the generalized stacking fault formation. The

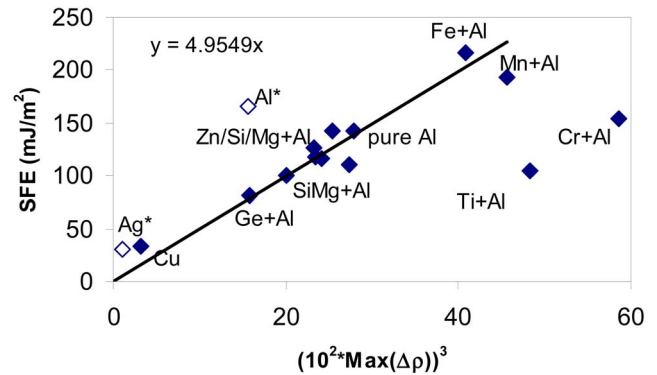


FIG. 3. (Color online) Correlation between the SFE and the maximum charge transfer  $\text{Max}(\Delta\rho_0)$  at the CDFP (the middle plane between the shifted and nonshifted atomic layers). The solid diamonds are results from our current calculations, and the open diamonds are estimated for Ag and Al from Ref. 28.

reported absolute charge difference is about  $0.075 \text{ eV}/\text{\AA}^3$  for Al and  $0.11 \text{ eV}/\text{\AA}^3$  for Ag, and after normalizing by the number of valence electrons, the values become  $0.025/\text{\AA}^3$  for Al and  $0.01/\text{\AA}^3$  for Ag. It also shows the same trend that larger charge transfer on the fault plane correlates to a higher SFE. Therefore the maximum value of charge difference on the fault plane,  $\text{Max}(\Delta\rho)$ , can be used to characterize how many electrons have been redistributed due to the stacking fault formation and will be also correlated with the value of the SFE.

The electron redistribution upon stacking fault formation not only indicates the directionality of the bonds of the atoms across the stacking fault, but also contributes most of the energy difference between the two systems (with and without stacking fault), which is taken as the SFE in this calculation. If there is no electron density difference after the atoms shift—i.e.,  $\text{Max}(\Delta\rho)=0$ —the energy change should be zero and the SFE should be zero. In Fig. 3, we compare  $\text{Max}(\Delta\rho)$  for all the Al systems with the solute atoms at the middle plane below the fault plane. There is a good correlation between the SFE and  $\text{Max}(\Delta\rho)$  as a cubic polynomial fitting was calculated going through the origin and most of the data points (except for Cr and Ti). This fitting is adequate, even for the other authors' calculations, which were not included in the fitting. We are not aware of any previous quantitative relationship between SFE and charge density. Since the charge density is a scalar field, changes in the SFE result from changes in the whole field, and the correlation between the charge density and the energy is not straightforward. The reason for this cubic relationship is not clear, but nevertheless it gives a hint as to how to relate the SFE to charge densities. A larger  $\text{Max}(\Delta\rho)$  indicates more electron shifting outside the atomic core, which again comes from the directional property of the bond.

If only the solute atoms segregated near the dislocation core are to be considered, the amount of solute needed for a typical deformed Al sample, that has a  $10^{11}$ – $10^{12} \text{ cm}/\text{cm}^3$  dislocation density, will be less than ppm level. In fact, preferential segregation of solutes on dislocations and the effect of ppm level Fe impurity in Al has been reported in the

literature.<sup>2</sup> In other words, a large amount of alloying solutes is not needed to change the deformation behavior of Al alloys through reduction of SFE. Our results suggest that Mg can lower the SFE and Fe can increase the SFE, which is consistent with experimental observations, and Ge alloying can further lower the SFE in Al about 42%. But no alloying addition has reduced the SFE of Al to a value as low as Cu. Therefore there may be a limitation to reducing the SFE by alloying. It has been indicated experimentally that Cr can also lower the SFE. The current results do not indicate this trend. Considering Cr did not follow the correction between SFE and charge density difference in Fig. 3 either, it may be necessary to include spin effects of Cr in future DFT calculations.

#### IV. SUMMARY

In summary, DFT has been used to calculate the SFE in binary and ternary alloys of Al with common alloying elements. The results show that electronic charge transfer at the stacking fault in the presence of the alloying element determines the change on the SFE due to alloying. The calcula-

tions also suggest that it is possible to alter the anisotropy of the electron distribution around Al atoms by alloying that could influence the slip behavior. These results provide a guideline for choosing solute additions to decrease the SFE and change the slip behavior in Al alloys.

To confirm these predictions, more experimental study of the dependence of slip behavior on alloying addition is needed. High-resolution transmission electron microscopy imaging<sup>12</sup> of dislocation core structure for edge dislocations in different binary alloys of Al can provide direct evidence of partials separated by stacking fault. Weak beam electron microscopy<sup>29</sup> of deformed binary Al alloys could reveal the two- and three-dimensional dislocation network formation and stacking fault tetrahedral with different alloying additions. And *in situ* nanoindentation experiments in the TEM<sup>30</sup> on binary alloys can be used to observe changes in dislocation network formation and slip behavior with alloying.

#### ACKNOWLEDGMENTS

The authors wish to thank Anil Sachdev, Y. T. Cheng, and Louis G. Hector, Jr. for helpful discussions.

\*Author to whom correspondence should be addressed. Electronic address: yue.qi@gm.com

<sup>1</sup>G. Schoeck, *Dislocations in Solids*, edited by F. R. N. Nabarro (North-Holland, Amsterdam, 1980), Vol. 3, pp. 63–163.

<sup>2</sup>S. Saimoto, S. Cao, and R. K. Mishra, *Mater. Sci. Forum* **475-479**, 421 (2005).

<sup>3</sup>J. R. Rice and G. E. Beltz, *J. Mech. Phys. Solids* **42**, 333 (1994).

<sup>4</sup>U. F. Kocks, U. F. Argon, and M. F. Ashby, *Prog. Mater. Sci.* **19**, 1 (1975).

<sup>5</sup>S. Ogata, J. Li, and S. Yip, *Science* **298**, 807 (2002).

<sup>6</sup>J. C. Grossman, A. Mizel, M. Cote, M. L. Cohen, and S. G. Louie, *Phys. Rev. B* **60**, 6343 (1999).

<sup>7</sup>J. P. Simon, *J. Phys. F: Met. Phys.* **9**, 425 (1979).

<sup>8</sup>S. M. Foiles, M. I. Baskes, and M. S. Daw, *Phys. Rev. B* **33**, 7983 (1996).

<sup>9</sup>F. Ercolessi and J. B. Adams, *Europhys. Lett.* **26**, 583 (1994).

<sup>10</sup>A. Asnalides and V. Pontikis, *Comput. Mater. Sci.* **10**, 401 (1998).

<sup>11</sup>G. Schoeck, *Mater. Sci. Eng., A* **333**, 390 (2002).

<sup>12</sup>W. Hollerbauer and P. Karnthaler, *Beitr. Elektronenmicr. Direktabb. Oberfl.* **14**, 361 (1981).

<sup>13</sup>W. Truszkowski, A. Pawlowski, and J. Dutkiewics, *Bull. Acad. Pol. Sci., Ser. Sci. Tech.* **19**, 55 (1979).

<sup>14</sup>M. J. Bull and S. Saimoto, in *Solute-Defect Interaction*, edited by S. Saimoto, G. Purdy, and G. Kidson (Pergamon, Toronto, 1986), pp. 375–381.

<sup>15</sup>G. Kresse and J. Hafner, *Phys. Rev. B* **49**, 14251 (1994).

<sup>16</sup>G. Kresse and J. Furthmüller, *Comput. Mater. Sci.* **6**, 15 (1996).

<sup>17</sup>J. P. Perdew, J. A. Chevary, S. H. Vosko, K. A. Jackson, M. R. Pederson, D. J. Singh, and C. Fiolhais, *Phys. Rev. B* **46**, 6671 (1992).

<sup>18</sup>A. M. Rappe, K. M. Rabe, E. Kaxiras, and J. D. Joannopoulos, *Phys. Rev. B* **41**, 1227 (1990).

<sup>19</sup>L. Kleinman and D. M. Bylander, *Phys. Rev. Lett.* **48**, 1425 (1987).

<sup>20</sup>D. Vanderbilt, *Phys. Rev. B* **41**, 7892 (1990).

<sup>21</sup>P. E. Blöchl, O. Jepsen, and O. K. Andersen, *Phys. Rev. B* **49**, 16223 (1994).

<sup>22</sup>R. P. Feynman, *Phys. Rev.* **56**, 340 (1939).

<sup>23</sup>W. H. Press, S. A. Teukolsky, W. T. Vetterling, and B. P. Flannery, *Numerical Recipes in Fortran 90: The Art of Parallel Scientific Computing*, 2nd ed. (Cambridge University Press, Cambridge, England, 1996).

<sup>24</sup>H. E. Swanson, *Standard X-ray Diffraction Powder Patterns*, Natl. Bur. Stand. U.S. Circ. No. 539 359, 1-1 (U.S. GPO, Washington, DC, 1953).

<sup>25</sup>G. Simmons and H. Wang, *Single Crystal Elastic Constants and Calculated Aggregate Properties: A Handbook*, 2nd ed. (MIT Press, Cambridge, MA, 1971).

<sup>26</sup>C. Kittel, *Introduction to Solid State Physics*, 7th ed. (Wiley, New York, 1996).

<sup>27</sup>G. Lu, D. Orlikowski, I. Park, O. Politano, and E. Kaxiras, *Phys. Rev. B* **65**, 064102 (2002).

<sup>28</sup>N. Kioussis, M. Herbranson, E. Collins, and M. E. Eberhart, *Phys. Rev. Lett.* **88**, 125501 (2002).

<sup>29</sup>M. Niewczas, *Philos. Mag. A* **82**, 393 (2002).

<sup>30</sup>A. M. Minor, S. A. S. Asif, Z. W. Shan, E. A. Stach, E. Cyranowski, T. J. Wyrobek, and O. L. Warren, *Nat. Mater.* **5**, 697 (2006).

<sup>31</sup>J. P. Hirth and J. Lothe, *Theory of Dislocations*, 2nd ed. (Wiley, New York, 1982).